SCIENTIFIC REPORTS

OPEN

SUBJECT AREAS:
MATERIALS SCIENCE
FERROELECTRICS AND MULTIFERROICS

Received
27 January 2014

Accepted
22 May 2014

Published
11 June 2014

Correspondence and requests for materials should be addressed to H.K. (kimura.hideo@nims.go.jp) or Z.X.C. (cheng@uow.edu.au)

Large magnetoelectric coupling in magnetically short-range ordered $Bi_5Ti_3FeO_{15}$ film

Hongyang Zhao[1,2], Hideo Kimura[2], Zhenxiang Cheng[3], Minoru Osada[2], Jianli Wang[3,4], Xiaolin Wang[3], Shixue Dou[3], Yan Liu[1], Jianding Yu[1], Takao Matsumoto[5], Tetsuya Tohei[5], Naoya Shibata[5] & Yuichi Ikuhara[5]

[1]State Key Laboratory of High Performance Ceramics and Superfine Microstructure, Shanghai Institute of Ceramics, Chinese Academy of Sciences, 1295 Dingxi Road, Shanghai 200050, China, [2]National Institute for Materials Science, Sengen 1-2-1, Tsukuba 305-0047, Japan, [3]Institute for Superconducting and Electronics Materials, University of Wollongong, Fairy Meadow, NSW 2519, Australia, [4]Bragg Institute, ANSTO, Lucas Heights, New South Wales 2234, Australia, [5]Institute of Engineering Innovation, School of Engineering, University of Tokyo, 2-11-16 Yayoi, Bunkyo-ku, Tokyo 113-8656, Japan.

Multiferroic materials, which offer the possibility of manipulating the magnetic state by an electric field or vice versa, are of great current interest. However, single-phase materials with such cross-coupling properties at room temperature exist rarely in nature; new design of nano-engineered thin films with a strong magneto-electric coupling is a fundamental challenge. Here we demonstrate a robust room-temperature magneto-electric coupling in a bismuth-layer-structured ferroelectric $Bi_5Ti_3FeO_{15}$ with high ferroelectric Curie temperature of ~1000 K. $Bi_5Ti_3FeO_{15}$ thin films grown by pulsed laser deposition are single-phase layered perovskit with nearly (00l)-orientation. Room-temperature multiferroic behavior is demonstrated by a large modulation in magneto-polarization and magneto-dielectric responses. Local structural characterizations by transmission electron microscopy and Mössbauer spectroscopy reveal the existence of Fe-rich nanodomains, which cause a short-range magnetic ordering at ~620 K. In $Bi_5Ti_3FeO_{15}$ with a stable ferroelectric order, the spin canting of magnetic-ion-based nanodomains *via* the Dzyaloshinskii-Moriya interaction might yield a robust magneto-electric coupling of ~400 mV/Oe·cm even at room temperature.

Multiferroic materials, such as those characterized by the coexistence of ferromagnetic and ferroelectric orders, have recently attracted ever-increasing interest and provoked a great number of research projects, driven by the intriguing physics and novel functionality resulting from the coupling between ferroelectric and magnetic orders[1–7]. The key feature of the multiferroic materials, the magnetoelectric (ME) effect, the coupling interaction between two ferroic orders, provides an additional degree of freedom in the design of novel multifunctional devices. It would be ideal if there is a single-phase multiferroic material with ME effect at room temperature, but unfortunately, they are very rare[8]. The large magnetoelectric coupling in a single-phase multiferroic material can be achieved by a spin-orbit coupling driven inverse Dzyaloshinskii–Moriya (DM) interaction between two neighbouring spins in spin-driven ferroelectric systems, as in helimagnets[2]. The asymmetric non-collinear spin configuration needed for the inverse DM interaction, however, usually only appears at very low temperature, which makes it useless for application at room temperature.

Extensive material engineering methods have been tried in order to develop novel multiferroic materials with large coupling intensity at room temperature, which include chemical substitution in the room-temperature (RT) ferroelectric antiferromagnet $BiFeO_3$[9], strain engineering[10], interface engineering (Fe/$BaTiO_3$)[11], and the combination of ferroelectric and ferromagnetic materials with high ordering temperatures to design composite (or "artificial") multiferroics, usually in the form of ceramics or self-organized nanostructures[12,13]. Very recently, the epitaxial $Bi_5Ti_3FeO_{15}$-$CoFe_2O_4$ multiferroic nanostructures were fabricated and shown how polarization and magnetism can be manipulated by stress in this system[14]. Unfortunately, such engineered ferroic/magnetoelectric behaviour is still limited by the coupling intensity, application temperature, and application suitability. Therefore, a practical room-temperature single phase ferroelectric ferromagnet with useful magnetoelectric coupling intensity remains elusive.

Recently, a novel class of materials with the general formula of $(Bi_2O_2)^{2+}(A_{m-1}B_mO_{3m+1})^{2-}$ (m: number of pseudo-perovskite layers) and an Aurivillius layer structure has come to our attention[15,16]. This class of compound is naturally ferroelectric at room temperature, with very high ferroelectric transition temperatures, such as

1021 K[17–19]. Importantly, the B sites of those Aurivillius compounds can accommodate elements with different valence states[20–25], making it possible to achieve the general formula of $Bi_4Ti_3O_{12}{\cdot}nBiMO_3$ (M = Fe, Mn; n = 1, 2), which creates the possibility of introducing novel properties not possessed by the parent compound, especially the capability for magnetic ion doping to introduce magnetic ordering and make the material multiferroic. Magnetic ions in $Bi_4Ti_3O_{12}{\cdot}nBiMO_3$ would be responsible for the observation of magnetism. The critical parameters determining the type of magnetism in terms of the exchange interaction are the local environment of the magnetic ions and the distance between neighbouring ions. Thermodynamically the system prefers random distribution of the ions, however if there is large different in their chemical properties of the ions, they will prefer to take ordered structure (ordered arrangement of ions in the structure), this arrange will reduce the energy of the whole system (lower entropy). For example, in some ordered structured materials[26], due to a big difference in Na^+ and Mn^{3+}, a site ordered structure can be formed. Due to the very large differences between Ti and other magnetic transition metal ions in terms of their chemical properties and sizes, magnetic ions have the possibility of being located at specific positions by replacing Ti to form an ordered atomic structure. In this case, the ordered transition metal atoms in the lattice will lead to the formation of a natural super-lattice with the layers in single-crystal unit-cell thickness in the form of a single $BiMO_3$ layer sandwiched by $Bi_4Ti_3O_{12}$ layers. This situation would make $Bi_4Ti_3O_{12}{\cdot}nBiMO_3$ a possible multiferroic at room temperature for M = Fe, considering that $BiFeO_3$ is a well-known room temperature multiferroic material. In addition to the most ideal case, there are three other possibilities for transition metal distribution in $Bi_4Ti_3O_{12}{\cdot}nBiMO_3$: Firstly, it can also exist as a precipitate of M-O compounds at the grain boundaries. That will make the material actually a composite containing two different chemical phases. All the measured properties, especially the magnetic properties, would actually result from a magnetic second phase. Secondly, M may be randomly distributed in the crystal lattice by replacing Ti to form some transition metal rich nano-regions, while the material is still in single phase. Magnetic ordering may occur in the transition-metal-rich area due to the shorter distance between adjacent transition metal ions. Due to the nature of the single phase, the magnetoelectric coupling can be quite large if there is any. Thirdly, the transition metal may be distributed homogenously in the crystal lattice, while there is no magnetic ordering because the distances between magnetic ions are too large, which makes the exchange interaction difficult to achieve.

It is quite obvious that how the magnetic ions are distributed in $Bi_4Ti_3O_{12}{\cdot}nBiMO_3$ is crucial for deciding the magnetism of the system, the possible multiferroic property, the magnetoelectric coupling, and the possible design of a new class of multiferroic materials. In this work, we fabricated $Bi_5Ti_3FeO_{15}$ ($Bi_4Ti_3O_{12}{\cdot}BiFeO_3$) (denoted as BTFO) film on $Pt/Ti/SiO_2/Si$ substrate using a pulsed laser deposition system (PLD), and investigated how the magnetic Fe ions are distributed in the crystal lattice and whether a magnetic ordering state can occur. In order to exclude the existence of a second ferromagnetic phase, as pointed out in the literature[27,28], we obtained a large field-of-view elemental mapping by using a scanning transmission electron microscope (STEM) X-ray energy dispersive spectroscopy (XEDS) imaging technique, as well as confirmation by X-ray diffraction (XRD). Then, we observed the atomic structure of single crystal grains, taking advantage of the state-of-the-art aberration-corrected STEM technology[29–32], and succeeded in obtaining very high resolution atomic images of the BTFO film. Finally, the ME coupling effect was confirmed in this material.

Results

Characterization of BTFO film. As shown in Figure 1, the film sample was examined by X-ray diffraction (XRD), which

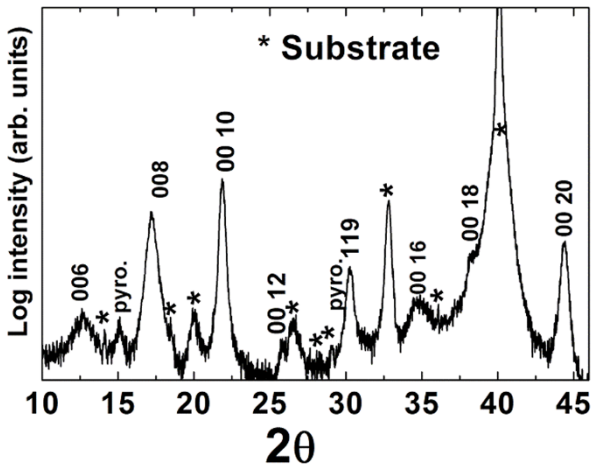

Figure 1 | XRD patterns of BTFO film deposited on $Pt/Ti/SiO_2/Si$ substrate, λ = 1.5406 Å.

demonstrates that the BTFO film can be indexed as a layered perovskite structure with space group $A2_1am$. There are two extra unidentified peaks in the XRD and they were indexed as the pyrochlore phase of $Bi_2Ti_2O_7$, which were shown in Figure 1 as Pyro. This feature is similar with the film obtained by PLD in another paper[33]. The phase of $Bi_2Ti_2O_7$ will not contribute to the ferroelectric properties for BTFO film. On the other hand, $Bi_2Ti_2O_7$ does not contain a magnetic transition metal, it will not affect the magnetic properties. In addition, the film is polycrystalline in nature, which makes a film with a certain thickness similar to its bulk form in physical properties. It has been found that our film is not fully *c*-oriented, but with a strong (119) diffraction. This is most probably due to a large lattice mismatch between BTFO and Pt substrate; such a lattice mismatching prohibits the *c*-oriented growth of BTFO. The microstructure of the film was observed in bright-field transmission electron microscope (TEM) images as shown in Figure 2, which proved the high quality of the film and its layered structure (also shown in Figure S1 in Supporting Information). The dark-field TEM image shown in the inset in Figure 2(b) exhibits a ferroelectric domain structure in a single grain. The atomic structure of the layered structure was further visualized by state-of-the-art aberration corrected scanning TEM high-angle annular dark-field (STEM HAADF) images, as shown in Figure 3. The image directly confirmed that there are three layers of Bi atoms $(Bi_3Ti_4O_{13})^{2-}$ sandwiched by two closely stacked Bi layers of $(Bi_2O_2)^{2+}$. Between the three layers of Bi atoms, individual columns of Ti/Fe atoms can be clearly recognized in this image viewed along the [110] direction of the crystal. A detailed analysis of the image suggested an atomic shift of the Ti/Fe columns from the central position between the two Bi_2O_3 columns, which appears as direct evidence of the ion-displacement driven ferroelectricity of the compound (see Figure S2).

Then, the distribution of Fe atoms in the lattice structure was analysed by the STEM energy dispersive X-ray spectroscopy (STEM-EDX) mapping technique, as shown in Figure 4. The direct evidence that no Fe_2O_3 nanoparticles could be observed by a large area scan excludes the origin of any magnetism from a second phase. Furthermore, our high resolution STEM-EDX mapping results showed no localized distribution of Fe atoms in a specific layer between the two Bi_2O_2 layers, although there was some degree of inhomogeneous distribution of Fe atoms. That is, Fe atoms in the film are not homogeneously distributed, but they do form some Fe-rich nano-regions. More scans of the elements in different areas of the thin film sample confirmed the existence of the Fe rich areas, but excluded the existence of Fe ordering in the single layer between two layers of Bi_2O_2. The same measurements on a bulk sample gave

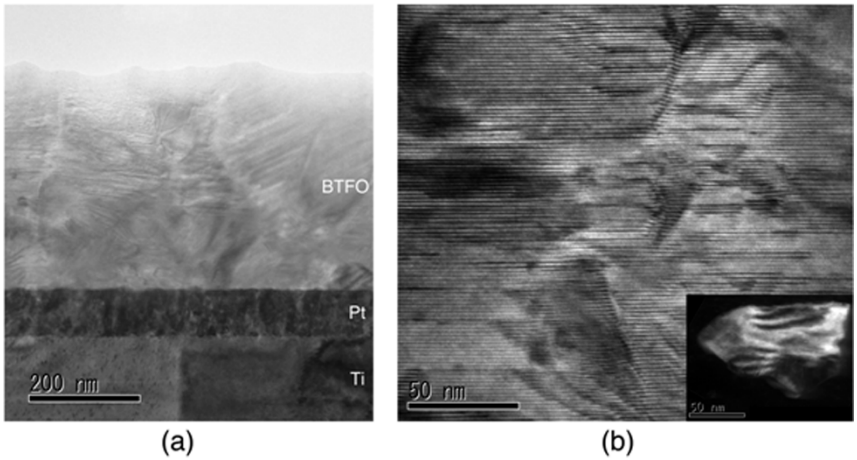

Figure 2 | **TEM images of BTFO film deposited on Pt/Ti/SiO_2/Si substrate.** A medium and a high magnification bright-field TEM image are shown in (a) and (b), respectively. In (b), the high quality of the layered structure is clearly visualized. In a dark-field TEM image, as shown in the inset, stripes corresponding to ferroelectric domains in a single grain can be observed.

similar results. Although this result is not the highly expected case, i.e., where Fe atoms are located in a single layer and form an ordered atomic structure, it is expected that such Fe-rich nano-regions could result in some kind of magnetic ordering and finally, magnetoelectric coupling. EDX results at grain boundary were also shown in Figure S3 in the Supporting Information.

Correlation between magnetism and structure. The magnetic properties of the BTFO film were carefully examined, as shown in Figure 5. Weak ferromagnetism is observed at room temperature, which is evidenced by a well saturated M-H loop with a saturated magnetic moment of ~8 emu/cm^3 (0.066 μ_B per unit cell) at room temperature (shown in the Figure 6 inset). Similar results on the weak ferromagnetic properties have been previously reported[33]. The Figure 5 inset shows the zero-field-cooled and field-cooled (ZFC-FC) curves above room temperature, where a weak ferromagnetic transition around 620 K is observed, which is close to the paramagnetic to spiral antiferromagnetic transition temperature of $BiFeO_3$ (~640 K)[34]. To confirm this observation, the same magnetic transition temperature (~620 K) was also observed in BTFO ceramics, as shown in Supporting Information Figure S4. To confirm that the abnormality in the magnetization is caused by the existence of long-range magnetic ordering, powder neutron diffraction was carried out across the temperature of the magnetic abnormality. Neutron powder diffraction (as shown in Figure S5 in the Supporting Information) of the ceramic sample shows that there is no new peak that appears around the magnetic transition temperature of ~620 K, but a clear abnormality in the peak intensity at around ~620 K is observed. This indicates that although there is no obvious long-range magnetic ordering, some kind of magnetic ordering does occur at that temperature. Mössbauer spectroscopy is a powerful and highly sensitive tool to detect magnetic ordering by monitoring the peak splitting and peak intensity. The Mössbauer spectra of BTFO ceramic sample at room temperature contain features consistent with quadrupolar effects (can be fitted by one doublet), which indicates the absence of long-range magnetic ordering (as shown in Figure S6). There might be a short-range magnetic ordering, however, from the Fe-rich areas in both the thin film and the bulk samples, where the Fe-rich areas mimic $BiFeO_3$, considering their very similar magnetic ordering temperature. In addition, the very small magnetic moment per unit cell of BTFO indicates a canted antiferromagnetic structure in

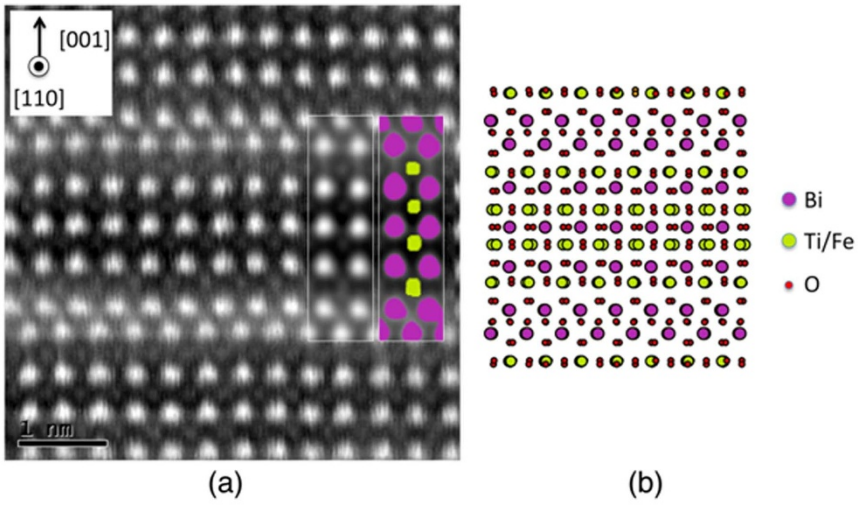

Figure 3 | HAADF STEM image (a) of a BTFO thin film obtained by the state-of-the-art aberration corrected STEM instrument, which shows three layers of Bi atoms $(Bi_3Ti_4O_{13})^{2-}$ sandwiched by two closely stacked Bi layers of $(Bi_2O_2)^{2+}$. Between the two $(Bi_2O_2)^{2+}$ layers, there are four Ti(Fe)O_6 octahedra. The insets show a typical image of the unit cell and its pseudo-colour representation. Individual columns of Bi and Ti/Fe atoms are clearly recognized. A schematic diagram of the Aurivillius structure of BTFO is shown in (b).

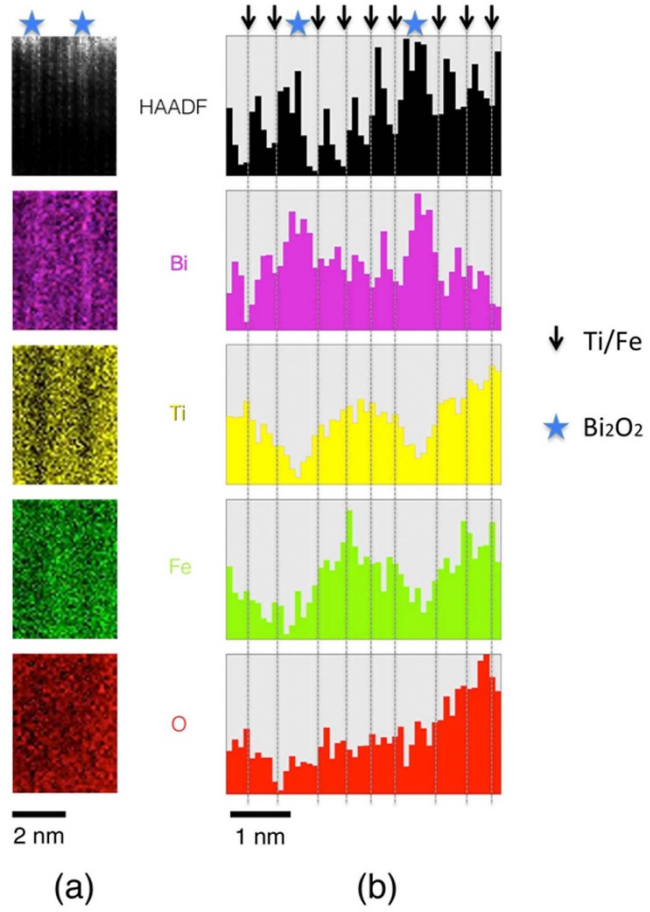

Figure 4 | STEM EDX mapping of a thin film specimen prepared from the deposited film. The average line profiles of the elemental mapping data as shown in (a) are presented in (b).

those Fe-rich nano-regions, which mimics $BiFeO_3$ to some extent. At low temperature, an enhancement of the magnetic moment on both the FC and the ZFC magnetization curves, accompanied by bifurcations between the FC and ZFC curves, were observed for all cooling fields of 500 Oe, 1 kOe, and 2 kOe, as indicated in Figure 5, but the bifurcation feature is largely suppressed at 5 kOe, and the temperature for this feature gradually decreases with increasing applied magnetic field. These observations indicate a spin-glass-like behaviour, which is similar to the case of $BiFeO_3$[35]. It arises from weak ferromagnetism, from the competition between the ferromagnetic and antiferromagnetic transitions in the thin film or from the spin frustration caused by strain effect at the film/substrate interface[36,37]. The spin configuration in the magnetic locally ordered BTFO and whether it keeps the same spiral structure as in $BiFeO_3$ are highly uncertain because investigating these aspects is beyond the ability of our current detection methods.

Characterization of ferroelectric domains and hysteresis loops. The ferroelectric domain structure of the thin film was studied. As is well known, the ferroelectric property is mainly determined by the domain structure and the domain wall motions. The coupling of the magnetic ordering with ferroelectric ordering will make the ferroelectric domain structure different from those in normal ferroelectric materials, which thus could allow judgement of any coupling effect. The ferroelectric domain morphology of the BTFO film was studied using piezoresponse force microscopy (PFM). Figure 7 shows the topography (a) and the corresponding in-plane (IP) PFM images ((b), (c)), and topography (d) and corresponding the out-of-plane (OP) PFM images ((e), (f)). Ferroelectric domain

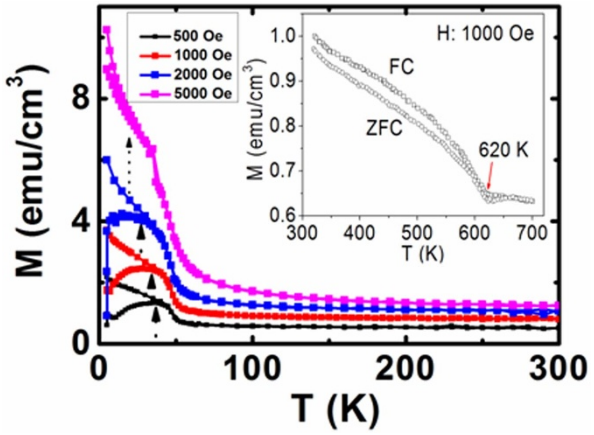

Figure 5 | ZFC-FC curves measured under different magnetic fields; inset shows high-temperature ZFC-FC curves at 1000 Oe.

switching over the polarized square after poling by ±6 V (IP) and ±10 V (OP) voltages was also observed, as shown in Supporting Information Figure S7. The contrast is due to the different phases of the PFM response for the up and down domains, and they confirm the polarization reversal in the sample. The presence of contrast in both the OP and the IP images indicates multiple orientations of grains and hence domains. Suppression of the OP response suggests a constrained ferroelectric domain-orientation along the IP direction. Figure 7 (g) shows an example of the local butterfly-type piezoresponse hysteresis loops. When a direct current voltage of up to 7 V was applied, the sample exhibited a typical "butterfly" loop. According to the equation, inverse piezoelectric coefficient $d_{33} = \Delta l/V$, where Δl is the displacement and V the voltage, the effective d_{33} could be calculated. At the voltage of 7 V, the sample shows effective $d_{33} \approx 22$ pm/V. The asymmetry is due to a self-poling effect which arises at the interface between the film and the bottom electrode.

It can be seen from the PFM images in Figure 7 that the spontaneous ferroelectric domains are irregular in shape. It should be noted that the domains in the BTFO film are bigger than normal ferroelectric domains. The domain period in BTFO film is close to 500 nm, which is comparable with the domain size of magnetic Co (400–600 nm)[38,39] and much larger than the ferroelectric domains in $BaTiO_3$ (100–150 nm)[40] with the same thickness. Usually, ferromagnetic domains are bigger than ferroelectric domains. In multiferroic materials, such big domain sizes usually suggest a high energy cost of

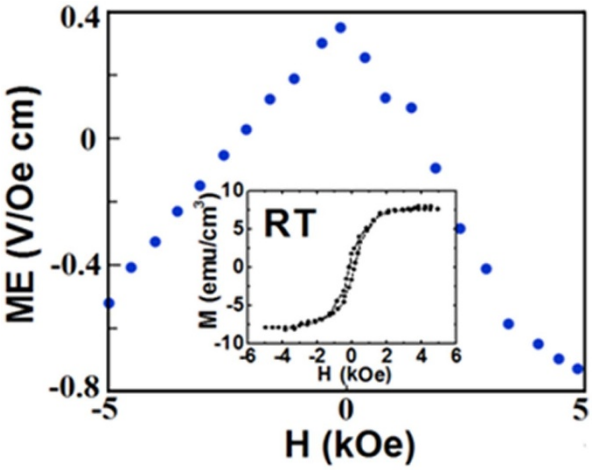

Figure 6 | ME coupling versus magnetic field; inset shows the magnetic hysteresis loop measured at room temperature. The magnetic field is normal to the thin film surface.

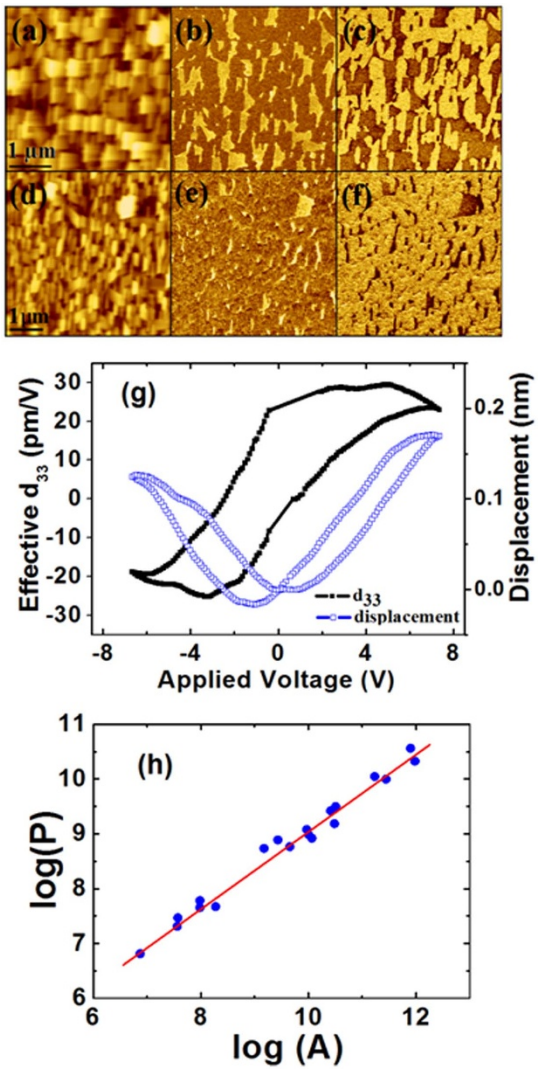

Figure 7 | (a–f) IP (top row) and OP (bottom row) topography with corresponding PFM images; (g) is the local piezoresponse versus applied voltage; (h) is the log-log plot of the domain perimeter as a function of area, with film thickness of 440 nm.

the domain walls and indicate a strong magnetoelectic coupling at the domain walls. The domains in multiferroics are thus very interesting, which is also consistent with previous results on magnetoelectric coupling at the domain walls[41]. The in-plane domains were characterized by a fractal dimension, as shown in Figure 7 (h). The domain perimeter (P) as a function of area (A) is plotted on a log-log scale using the program WSxM[42]. The ratio of P to A can be analysed using $P \propto A^{H_{||}/2}$, where $H_{||}$ is the in-plane Hausdorff dimension of the domain walls. The value of $H_{||}$ should be in the range of $1 \leq H_{||} \leq 2$. The smaller the $H_{||}$ value, the smoother the domain walls will be, and $H_{||}$ has the value of 1 if the domain walls are perfectly smooth. The slope of the log(P) vs. log(A) plot for the domains in the BTFO film was found to be 1.44, which is within the range of $BiFeO_3$ films with values of $1.29 \leq H_{||} \leq 1.52$[41]. The similar $H_{||}$ values for the BTFO film and $BiFeO_3$ indicate that they may share a similar magnetoelectric coupling mechanism.

The ferroelectric hysteresis loops of BTFO film were shown in Figure 8. The inset (b) and (c) show the fatigue properties. Judging from the P-E loops, the sample is relatively leaky, therefore positive-up-negative-down (PUND) measurement was carried out. Obvious switchable polarization was observed (as shown in Figure S8 in Supporting Information). All these measurements, the ferroelectric domain observation, domain switching behaviour, the switchable

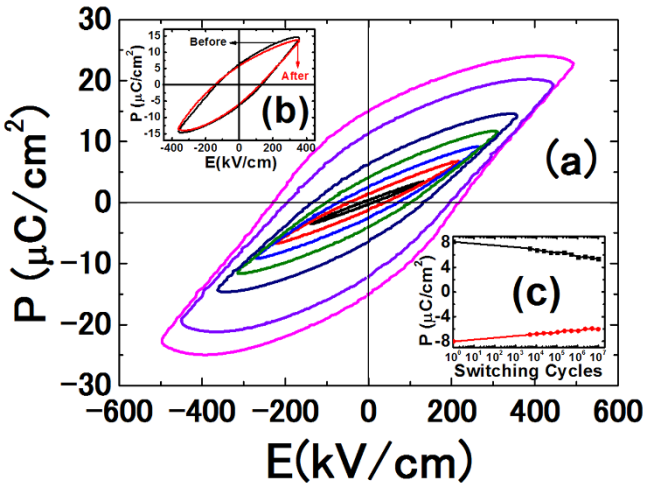

Figure 8 | (a) Ferroelectric hysteresis loops measured at room temperature at a frequency of 100 Hz, (b) and (c) show the fatigue properties of BTFO film.

polarization detected in PUND measurements, and P-E loops confirmed the ferroelectric property of the BTFO film.

Magnetodielectricity and magnetic field control of electric polarization. In order to test for any magnetoelectric coupling aroused by such short-ranged magnetic ordering, polarization-electrical field (P-E) loops from direct measurements of BTFO films in different magnetic fields at the temperatures of 10 K, 50 K, 100 K, and 300 K were collected as shown in Figure 9. A continuous increase in electric polarization (P) values can be observed until the applied magnetic field reaches a maximum for the temperatures studied. This is indicative of coupling between the two ordered ferroic parameters, especially at low temperature. The increase in the electric polarization in magnetic field can reach a value of 574%, with a real P = of 77.5 μC/cm² in 1 Tesla magnetic field at 10 K, which is defined as $P_{ME} = (P_H - P_0)/P_0 = 574\%$, where P_H and P_0 are the polarizations measured with and without magnetic field, respectively. Note that the reported value of the ferroelectric polarization of BTFO is $P_r \approx 13$ μC/cm² [43]. In addition, a strong nonlinear magnetic field dependence of the electric polarization is observed, which is evidenced by the sudden increase in the electric polarization at around 6500 Oe, which is more obvious at 10 K. This result shows the presence of a magnetic field induced polarization at room temperature, while the drastic enhancement of the polarization driven by magnetic field at 10 K may follow a mechanism different from what happens at room temperature. An increase in the dielectric constant as a function of magnetic field at 10 kHz was observed at room temperature and is shown as Figure 10 (with the inset showing the typical frequency dependence of the dielectric constant and dielectric loss under zero magnetic field). A magnetodielectric effect occurs, with a percentage value as great as 5.4%, which is defined by the percentage change in the dielectric constant, $\varepsilon_{ME} = (\varepsilon_H - \varepsilon_0)/\varepsilon_0$, where ε_H and ε_0 are the dielectric constant values in magnetic field and in zero magnetic field, respectively. This is another signature of the ME conversion occurring at room temperature in the sample. The room temperature ME coefficient, determined through direct measurement of the magnetic field induced electric voltage in the thin film, has a value of ~400 mV/(Oe·cm) at H = 0, as is shown in Figure 6, which is three orders of magnitude higher than in the previous report of a value of 0.1 $mVcm^{-1}Oe^{-1}$ in a ceramic sample[25]. The value is also nearly two orders of magnitude higher than that in a ceramic sample which was reported recently with the ME coefficient of 8.28 $mVcm^{-1}Oe^{-1}$ [43]. For the large difference for our film and

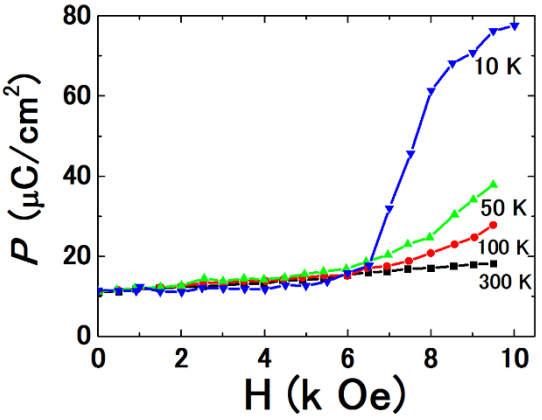

Figure 9 | Electric polarization versus magnetic field measured at the temperatures of 10 K, 50 K, 100 K, and 300 K. The magnetic field is normal to the film surface.

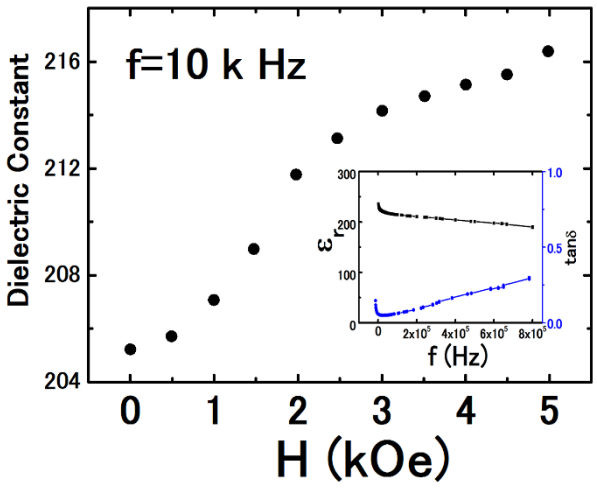

Figure 10 | Dielectric response in magnetic field measured at room temperature at a frequency of 10 kHz. The inset is the curve of the dielectric constant and dielectric loss versus frequency at zero magnetic field. The magnetic field is normal to the thin film surface.

ceramics, there are two reasons, one is the pure and good crystalline BTFO phase in the film sample; the other reason is strain which may cause a large difference between film and ceramics. This is direct evidence showing the possibilities for magnetic field control and switching of the electrical polarization at room temperature in BTFO film.

Discussion

The magnetoelectric coupling in BTFO film is regarded as driven by the inverse Dzyaloshinskii–Moriya (DM) interaction in the form of $\vec{P} = \alpha \sum_{ij} \overrightarrow{e_{ij}} \times \left(\vec{S}_i \times \vec{S}_j\right)$, where e_{ij} is the unit vector connecting the neighbouring spins S_i and S_j, and the proportionality constant α is determined by the spin–orbit and spin-exchange interactions, as well as the possible spin-lattice coupling term[2]. For example a non-zero value of the polarization P along the vertical direction requires mutually canted adjacent atomic sites and broken horizontal mirror-plane symmetry. Such a polarization can be easily controlled by an external magnetic field in a specific direction, as evidenced by the generation and/or flipping of the spontaneous polarization. Although the exact spin-ordering structure of the Fe-rich nano-regions in BTFO is not clear, the weak magnetic moment indicates a canted antiferromagnetic ordering. Such a canted antiferromagnetic structure can induce an electric polarization based on the above inverse DM interaction, which will be added to the dominant ion-displacement driven ferroelectric polarization. Therefore, at low and room temperature, only part of the polarization will show a response to external magnetic field. This part of polarization, which is driven by spin (canted antiferromagnetism), can be flipped by magnetic field (as evidenced by direct ME coupling measurements). The polarization may also be enhanced by magnetic field though complete spin-orbit-lattice coupling when the magnetic field works on spin (as evidenced by magneto-polarization measurements). Due to the polycrystalline nature of BTFO film, we cannot separate out how the magnetic field will affect the polarization by current measurements, i.e., flipping or enhancement, or even both. In addition, further studies like leakage property and dielectric loss under magnetic field and different temperature to exclude the possible reason of ME response, should be carried out in depth although now it is very difficult for us.

The introduction of magnetic Fe ions into Aurivillius layer-structured bismuth titanate forms some iron-rich nano-regions inside single grains. Such iron rich areas show a short-range magnetic ordering with a detectable transition temperature of ~620 K. Although long-range magnetic ordering is not formed at room temperature, magnetoelectric coupling is observed and has been confirmed by magneto-polarization, magnetodielectric, direct magnetoelectric coupling, and ferroelectric domain observations. The introduction of iron is not only the reason for the observed room temperature ME coupling, but also the reason for the enhancement in ferroelectric polarization. Therefore, short-range magnetic ordering is proposed for the first time as an origin of magnetoelectric coupling in Aurivillius layer-structured bismuth titanate. This novel concept will broaden the number of candidates that can show a magnetoelectric coupling effect for room temperature application. For example, by simply doping some magnetic ions into a ferroelectric host material which has very large chemical solubility, a single phase magnetoelectric material could be designed if there is no impurity formation. As BTFO shows a ferroelectric transition starting from a temperature much higher than the magnetic transition temperature, the ferroelectric polarization in BTFO at room temperature is not entirely driven by spin. The component of spin-driven polarization in the thin film becomes dominant, however, at low temperature due to changes in the spin configuration, as evidenced by both the significant enhancement of electric polarization and the magnetic transition that occurs around 50 K. In low magnetic field, the system will have a strong response to external magnetic field (magnetization process and thus caused ME) for such a short range order system. At the large magnetic field, the system gets saturated and the response to external magnetic field will become weak.

In summary, the origin of the room-temperature multiferroic properties in BTFO has been investigated by an analysis of the relationships among the microstructure and magnetism, magneto-polarization, magneto-dielectricity. The Fe atoms are not formed as a single layer in the interesting super-lattice microstructures; instead, there are some special Fe-rich nano-regions which contribute to the short-range magnetic ordering. Moreover, the magnetism, magneto-polarization and magneto-dielectricity are originated from the short-range magnetic ordering. It is expected that a higher concentration of iron may shorten the distance between iron ions and help in the formation of long-range magnetic ordering, eventually promoting larger spin-driven polarization and stronger ME coupling at room temperature.

Methods

BTFO films were deposited using pulsed laser deposition (PLD) on Pt/Ti/SiO_2/Si substrates. BTFO targets were 5–10% Bi-enriched sintered ceramics. The growth took place at the temperature of 520°C and under an oxygen pressure of 120 mTorr. XRD patterns were collected by a JEOL 3500 with Cu K_α radiation. The obtained thin film is around 400 nm in thickness.

The ferroelectric properties were measured at room temperature using an aixACCT EASY CHECK 300 ferroelectric tester and a RT6000 HVS test system

(Radiant Technologies). Pt upper electrodes with an area of 0.0314 mm^2 were deposited by magnetron sputtering through a metal shadow mask. The dielectric properties were measured using a HP4248 LCR meter and a precision impedance analyser (Agilent Technologies 4294A). The ferroelectric domain morphology was studied by piezoresponse atomic force microscopy (PFM). AnAC signal with amplitude of 1.5 V and frequency of 8 kHz was applied between the atomic force microscope (AFM) tip and the bottom electrode of the sample to acquire the piezo-response images. Nanotec's WsXM software was used to analyze the PFM images.

Magnetic measurements were performed using a magnetic properties measurement system (MPMS, Quantum Design). All of the curves shown in this letter are corrected to eliminate the diamagnetic background of the substrate, which was obtained from the same MPMS system.

The Magneto electric (ME) effect of was performed by using a Dynamic Magnetoelectric coupling measurement setup[44,45]. A Keithley 6221 ac source was used to supply the constant amplitude ac current to the solenoid to generate a 5 Oe ac magnetic field $h(f)$ with the frequency from dc to 100 kHz. A lock-in amplifier is employed to detect the induced ME voltage $V(f)$ across the sample thickness (d) with the same frequency of the ac current source. The background voltage noise due to the Faraday's Law has been successfully reduced to a very small level (below several microvolts) by a careful design of the voltage detecting circuit with twisting and electric field shielding. The high signal-to-noise ratio can guarantee the accuracy of our measurements. The ac magnetic field was applied parallel to the direction of the induced ME voltage, i.e., in a longitudinal mode. The linear ME coefficient α is defined as $\alpha = \frac{\delta E}{\delta H} = \frac{V_0(f)}{h_0(f)} \times \frac{1}{d}$.

Thin films for TEM/STEM observations were prepared by conventional mechanical grinding followed by Ar ion-beam milling using an Ion Slicer (IS, model EM-09100IS, JEOL, Ltd.) and a Precision Ion Polisher System (PIPS, Gatan, Inc.). Prior to TEM/STEM observations, the thin films were further polished with a low-voltage and low-angle Ar ion beam milling apparatus (model 1010, Fischione, Inc.). For TEM observations, we used a JEM-2010HC (JEOL, Ltd.). STEM observations were performed using a JEM-2100F with a probe-forming Cs corrector (CEOS, GmbH), and elemental analysis was performed in combination with a JEOL EX-24065 X-ray detector.

1. Hur, N. *et al.* Electric polarization reversal and memory in a multiferroic material induced by magnetic fields. *Nature* **429**, 392–395 (2004).
2. Kimura, T. *et al.* Magnetic control of ferroelectric polarization. *Nature* **426**, 55–58 (2003).
3. Alexe, M. *et al.* Ferroelectric Switching in Multiferroic Magnetite (Fe_3O_4) Thin Films. *Adv. Mater.* **21**, 4452–4455 (2009).
4. Catalan, G. & Scott, J. F. Physics and Applications of Bismuth Ferrite. *Adv. Mater.* **21**, 2643–2485 (2009).
5. Wang, J. *et al.* Epitaxial $BiFeO_3$ multiferroic thin film heterostructures. *Science* **299**, 1719–1722 (2003).
6. Nan, C. W. Magnetoelectric effect in composites of piezoelectric and piezomagnetic phases. *Phys. Rev. B* **50**, 6082–6088 (1994).
7. Spaldin, N. A., Cheong, S. W. & Ramesh, R. Multiferroics: Past, present and future. *Physics Today* **63**, 38–43 (2010).
8. Hill, N. A. Why are there so few magnetic ferroelectrics? *J. Phys. Chem. B* **104**, 6694–6709 (2000).
9. Cheng, Z. X., Wang, X. L., Dou, S. X., Kimura, H. & Ozawa, K. Enhancement of ferroelectricity and ferromagnetism in rare earth element doped $BiFeO_3$. *J. Appl. Phys.* **104**, 116109 (2008).
10. Macmanus-Driscoll, J. L. *et al.* Strain control and spontaneous phase ordering in vertical nanocomposite heteroepitaxial thin films. *Nature Mater.* **7**, 314–320 (2008).
11. Bocher, L. *et al.* Atomic and Electronic Structure of the $BaTiO_3$/Fe Interface in Multiferroic Tunnel Junctions. *Nano Lett.* **12**, 376–382 (2012).
12. Nan, C. W., Li, M. & Huang, J. H. Calculations of giant magnetoelectric effects in ferroic composites of rare-earth–iron alloys and ferroelectric polymers. *Phys. Rev. B* **63**, 155515 (2001).
13. Zheng, H. *et al.* Multiferroic $BaTiO_3$-$CoFe_2O_4$ Nanostructures. *Science* **303**, 661–663 (2004).
14. Imai, A. *et al.* Epitaxial $Bi_5Ti_3FeO_{15}$ - $CoFe_2O_4$ pillar-matrix multiferroic nanostructures. *ACS Nano* **7**, 11079–11086 (2013).
15. Cheng, Z. X., Wang, X. L., Zhao, H. Y. & Kimura, H. Lead-free potassium bismuth titanate thin film with complex Aurivillius layer structure. *J. Appl. Phys.* **107**, 084105 (2010).
16. Cheng, Z. X., Wang, X. L., Dou, S. X., Ozawa, K. & Kimura, H. Ferroelectric properties of $Bi_{3.25}Sm_{0.75}V_{0.02}T_{2.98}O_{12}$ thin film at elevated temperature. *Appl. Phys. Lett.* **90**, 222902 (2007).
17. Nakashima, S. *et al.* Structural and ferroelectric properties of epitaxial $Bi_5Ti_3FeO_{15}$ and natural-superlattice-structured $Bi_4Ti_3O_{12}$–$Bi_5Ti_3FeO_{15}$ thin films. *J. Appl. Phys.* **108**, 074106 (2010).
18. Li, J. B. *et al.* Ferroelectric transition of Aurivillius compounds $Bi_5Ti_3FeO_{15}$ and $Bi_6Ti_3Fe_2O_{18}$. *Appl. Phys. Lett.* **96**, 222903 (2010).
19. Suzuki, M., Nagata, H., Ohara, J., Funakubo, H. & Kakenaka, T. $Bi_{3-x}M_xTiTaO_9$ (M = La or Nd) ceramics with high mechanical quality factor Qm. *Jpn. J. Appl. Phys.* **42**, 6090–6093 (2003).
20. Aurivillius, B. Mixed bismuth oxides with layer lattices. *Ark. Kemi* **1**, 463–480 (1949).
21. Noguchi, Y., Miyayama, M. & Kudo, T. Direct evidence of *A*-site-deficient strontium bismuth tantalate and its enhanced ferroelectric properties. *Phys. Rev. B* **63**, 214102 (2001).
22. Wang, C. M. & Wang, J. F. High performance Aurivillius phase sodium-potassium bismuth titanate lead-free piezoelectric ceramics with lithium and cerium modification. *Appl. Phys. Lett.* **89**, 202905 (2006).
23. Noguchi, Y., Murata, K. & Miyayama, M. Effects of Defect Control on the Polarization Properties in Bi_2WO_6-Based Single Crystals. *Ferroelectrics* **355**, 55–60 (2007).
24. Noguchi, Y., Miyayama, M. & Kudo, T. Ferroelectric properties of intergrowth $Bi_4Ti_3O_{12}$–$SrBi_4Ti_4O_{15}$ ceramics. *Appl. Phys. Lett.* **77**, 3639 (2000).
25. Srinivas, A., Suryanarayana, S. V., Kumar, G. S. & Kumar, M. M. Magnetoelectric measurements on $Bi_5FeTi_3O_{15}$ and $Bi_6Fe_2Ti_3O_{18}$. *J. Phys.: Condens. Mat.* **11**, 3335–3340 (1999).
26. Zhang, S. *et al.* Site-selective doping effect in $AMn_3V_4O_{12}$ (A = Na^+, Ca^{2+}, and La^{3+}). *J. Am. Chem. Soc.* **135**, 6056–6060 (2013).
27. Zhang, P. F., Deepak, N., Keeney, L., Pemble, M. E. & Whatmore, R. W. The structural and piezoresponse properties of *c*-axis-oriented Aurivillius phase $Bi_5Ti_3FeO_{15}$ thin films deposited by atomic vapor deposition. *Appl. Phys. Lett.* **101**, 112903 (2012).
28. Keeney, L. *et al.* Room temperature electromechanical and magnetic investigations of ferroelectric Aurivillius phase $Bi_5Ti_3(Fe_xMn_{1-x})O_{15}$ (x = 1 and 0.7) chemical solution deposited thin films. *J. Appl. Phys.* **112**, 052010 (2012).
29. Haider, M. *et al.* Electron microscopy image enhanced. *Nature* **392**, 768–769 (1998).
30. Nellist, P. D. *et al.* Direct sub-angstrom imaging of a crystal lattice. *Science* **305**, 1741 (2004).
31. Shibata, N. *et al.* Atomic-scale imaging of individual dopant atoms in a buried interface. *Nature Mat.* **8**, 654–658 (2009).
32. Tohei, T. *et al.* Direct imaging of doped fluorine in $LaFeAsO_{1-x}F_x$ superconductor by atomic scale spectroscopy. *Appl. Phys. Lett.* **95**, 193107 (2009).
33. Nakashima, S., Nakamura, Y., Yun, K. Y. & Okuyama, M. Preparation and Characterization of Bi-Layer-Structured Multiferroic $Bi_5Ti_3FeO_{15}$ Thin Films Prepared by Pulsed Laser Deposition. *Jpn. J. Appl. Phys.* **46**, 6952–6955 (2007).
34. Cheng, Z. X., Wang, X. L., Dou, S. X., Ozawa, K. & Kimura, H. Improved ferroelectric properties in multiferroic $BiFeO_3$ thin films through La and Nb codoping. *Phys. Rev. B* **77**, 092101 (2008).
35. Singh, M. K., Katiyar, R. S., Prelier, W. & Scott, J. F. Almeida-Thouless line in $BiFeO_3$: Is Bismuth Ferrite a mean-field spin glass? *J. Phys.: Condens. Matter* **21**, 042202 (2009).
36. Venkatesan, S., Daumont, C., Kooi, B. J., Noheda, B. & Hosson, De Jeff Th. M. Nanoscale domain evolution in thin films of multiferroic $TbMnO_3$. *Phys. Rev. B* **80**, 214111 (2009).
37. Venkatesan, S. *et al.* Monodomain strained ferroelectric $PbTiO_3$ thin films: Phase transition and critical thickness study. *Phys. Rev. B* **78**, 104112 (2008).
38. Hehn, M., Padovani, S., Ounadjela, K. & Bucher, J. P. Nanoscale magnetic domain structures in epitaxial cobalt films. *Phy. Rev. B* **54**, 3428 (1996).
39. Catalan, G., Scott, J. F., Schilling, A. & Gregg, J. M. Wall thickness dependence of the scaling law for ferroic stripe domains. *J. Phys. Condens. Matter.* **19**, 022201 (2007).
40. Schilling, A. *et al.* Scaling of domain periodicity with thickness measured in $BaTiO_3$ single crystal lamellae and comparison with other ferroics. *Phy. Rev. B* **74**, 024115 (2006).
41. Catalan, G. *et al.* Fractal dimension and size scaling of domains in thin films of multiferroic $BiFeO_3$. *Phys. Rev. Lett.* **100**, 027602 (2008).
42. http://www.nanotec.es; Horcas, I. *et al. Rev. Sci. Instrum.* **78**, 013705 (2007).
43. Dercz, J., Bartkowska, J., Dercz, G., Stoch, P. & Lukasik, M. Effect of previous milling of precursors on magnetoelectric effect in multiferroic $Bi_5Ti_3FeO_{15}$ ceramic. *Int. J. Thermophys.* **34**, 567–574 (2013).
44. Mahesh Kumar, M., Srinivas, A., Suryanarayana, S. V., Kumar, G. S. & Bhimasankaram, T. An experimental setup for dynamic measurement of magnetoelectric effect. *Bull. Mater. Sci.* **21**, 251–255 (1998).
45. Zou, T., Wang, F., Liu, Y., Yan, L. Q. & Sun, Y. Multiferroicity and magnetoelectric coupling in half-doped manganite $La_{0.5}Ca_{0.5}MnO_3$. *Appl. Phys. Lett.* **97**, 092501 (2010).

Acknowledgments

The authors gratefully acknowledge Dr. Kazuya Terabe and Dr. Hideaki Kitazawa in the National Institute for Materials Science (NIMS), Japan for their help with experiments. Author Z.X. Cheng thanks ARC for support through a Future Fellowship. The authors acknowledge Mrs. M. Nakabayashi at the Green Network of Excellence (GRENE) for thin film preparation. A part of this work was conducted in the Research Hub for Advanced Nano Characterization, The University of Tokyo, supported by the Ministry of Education, Culture, Sports, Science and Technology (MEXT), Japan. A part of this work was conducted in GRENE and supported by the "Nanotechnology Platform" (project No. 12024046) both sponsored by MEXT, Japan. Author H.Y. Zhao thanks SICCAS for support through Y32ZC1110G and Y22ZB1110G. The authors thank Dr. Tania Silver for critical reading of this manuscript.

Author contributions

H.Y.Z., H.K. and Z.X.C. planned the project. H.Y.Z. prepared the sample. H.Y.Z., H.K., Z.X.C. and M.O. characterized the electrical properties. T.M., T.T., N.S. and Y.I. performed TEM analysis. J.L.W. performed neutron diffraction. X.L.W., S.X.D., Y.L. and Y.D. contributed to analysis. H.Y.Z., H.K. and Z.X.C. prepared the manuscript. All the authors contributed to revising the manuscript.

Additional information

Supplementary information accompanies this paper at http://www.nature.com/scientificreports

Competing financial interests: The authors declare no competing financial interests.

How to cite this article: Zhao, H.Y. *et al.* Large magnetoelectric coupling in magnetically short-range ordered $Bi_5Ti_3FeO_{15}$ film. *Sci. Rep.* **4**, 5255; DOI:10.1038/srep05255 (2014).

This work is licensed under a Creative Commons Attribution-NonCommercial-NoDerivs 4.0 International License. The images or other third party material in this article are included in the article's Creative Commons license, unless indicated otherwise in the credit line; if the material is not included under the Creative Commons license, users will need to obtain permission from the license holder in order to reproduce the material. To view a copy of this license, visit http://creativecommons.org/licenses/by-nc-nd/4.0/